

AD-A168 925

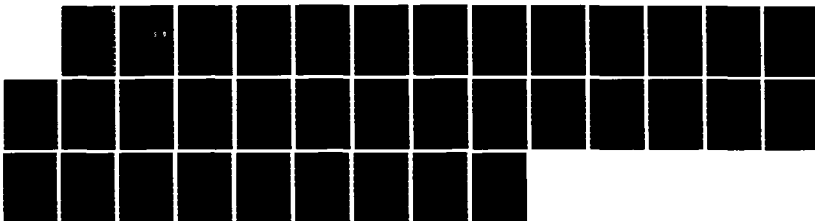
FRAGMENTATION DYNAMICS OF ENERGETIC MATERIALS(U)  
CORNELL UNIV ITHACA NY DEPT OF CHEMISTRY E R GRANT  
13 MAY 86 DAAG29-83-C-0020

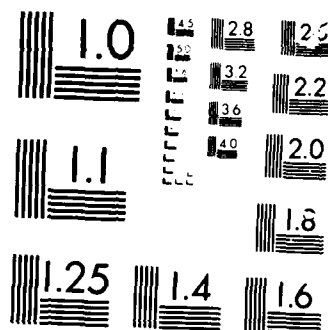
1/1

UNCLASSIFIED

F/G 7/5

NL





MICROCOPY

11/1/31

ARJ 19923.16-CH

(2)

AD-A168 925

FRAGMENTATION DYNAMICS OF ENERGETIC MATERIALS

FINAL REPORT

Edward R. Grant

May 13, 1986

U. S. Army Research Office

DAAG29-83-C-0020

Cornell University

DTIC  
ELECTE  
JUN 25 1986  
S D

FILE COPY

Approved for Public Release  
Distribution Unlimited

Unclassified

SECURITY CLASSIFICATION OF THIS PAGE (When Data Entered)

REPORT DOCUMENTATION PAGE		READ INSTRUCTIONS BEFORE COMPLETING FORM
1. REPORT NUMBER	2. GOVT ACCESSION NO.	3. RECIPIENT'S CATALOG NUMBER
4. TITLE (and Subtitle) Fragmentation Dynamics of Energetic Materials		5. TYPE OF REPORT & PERIOD COVERED FINAL 1/10/83 - 1/9/86
		6. PERFORMING ORG. REPORT NUMBER
7. AUTHOR(s) Edward R. Grant		8. CONTRACT OR GRANT NUMBER(s) DAAG29-83-C-0020
9. PERFORMING ORGANIZATION NAME AND ADDRESS Cornell University Department of Chemistry Ithaca, New York 14853		10. PROGRAM ELEMENT, PROJECT, TASK AREA & WORK UNIT NUMBERS
11. CONTROLLING OFFICE NAME AND ADDRESS U. S. Army Research Office Post Office Box 12211 Research Triangle Park, NC 27709		12. REPORT DATE May 13, 1986
		13. NUMBER OF PAGES
14. MONITORING AGENCY NAME & ADDRESS (if different from Controlling Office)		15. SECURITY CLASS. (of this report)  Unclassified
		15a. DECLASSIFICATION/DOWNGRADING SCHEDULE
16. DISTRIBUTION STATEMENT (of this Report)  Approved for public release; distribution unlimited.		
17. DISTRIBUTION STATEMENT (of the abstract entered in Block 20, if different from Report)  NA		
18. SUPPLEMENTARY NOTES  The view, opinions, and/or findings contained in this report are those of the author(s) and should not be construed as an official Department of the Army position, policy, or decision, unless so designated by other documentation		
19. KEY WORDS (Continue on reverse side if necessary and identify by block number) Energetic Materials , Alkyl Epoxides Unimolecular Decomposition , Molecular Beams Primary Reactions , Infrared Multiphoton Dissociation Nitro Paraffins , Multiphoton Ionization) Nitramines		
20. ABSTRACT (Continue on reverse side if necessary and identify by block number)  ➤ A molecular beam unimolecular fragmentation mass spectrometer has been developed and applied to the study of primary dissociation processes in energetic materials. The experimental approach uses infrared multiphoton excitation to prepare isolated molecules in the beam for dissociation. Visible laser induced multiphoton ionization detects products with time-of-flight scattering angle		

## TABLE OF CONTENTS

INTRODUCTION	1
PROGRESS REPORT	2
1. Fragmentation Kinetics and Dynamics of Energetic Reactions	3
2. New Diagnostics for Energetic Fragments	14
NO <sub>2</sub> : Non-Franck-Condon Two-photon Spectroscopy	14
Dynamical Jahn-Teller Effects in 3s <sup>1</sup> E' Sym-triazine	17
3. Multiresonant Spectroscopy and Intramolecular Dynamics	21
4. Dynamics of State-Selected Two-Photon Photofragmentation	24
5. Thermal Unimolecular Kinetics by Pulsed Molecular Beam Pyrolysis	26
REFERENCES	29
PARTICIPATING SCIENTIFIC PERSONNEL	31

Accession For	
NTIS	<input checked="" type="checkbox"/>
CRA&I	<input type="checkbox"/>
DTIC	<input type="checkbox"/>
TAB	<input type="checkbox"/>
Unannounced Justification	
By	
Distribution/	
Availability Codes	
Dist	Avail and/or Special
A-1	



## INTRODUCTION

Virtually all reactive energetic processes begin with the elementary chemical step of unimolecular decomposition. The early kinetics of even complex detonation reactions depend critically on the nature of initiating and propagating dissociative events. It follows that the construction of accurate rate models for chemically evolving energetic systems with widely and rapidly varying conditions of local temperature and pressure, demands a thorough theoretical understanding of key dissociative steps. To obtain direct experimental information on the course of fast-reacting energetic systems, one needs temporally precise, sensitive, and species-specific diagnostics.

Our laboratory has made advances in the areas of both fundamental unimolecular reaction dynamics and new laser-based diagnostics. Experimental work has centered on multiphoton ionization (MPI) as a method for spectroscopic identification and trace analysis.<sup>1-32</sup> Here photoion mass resolution ensures specificity, while newer two-color double resonant spectroscopic approaches introduce distinctive frequency signatures<sup>20</sup> and enlarge Franck-Condon envelopes for electronic transitions.<sup>21-25</sup> To study unimolecular kinetics and dynamics we have refined the technique of infrared laser induced multiphoton dissociation in molecular beams to yield direct information on unimolecular lifetimes together with fragment recoil velocities and internal state distributions.<sup>26-29</sup> Similar techniques are now being applied in our laboratory for UV photolysis, and we have found that optical selection of individual quantum states via intermediate resonance in two-photon photodissociation provides an exceptionally rich source of information on the quantum dynamics of photofragmentation.<sup>30-32</sup>

Current work is refining methods for characterizing the energy distribu-

tions of vibrationally excited products produced following infrared multi-photon dissociation by means of hot absorption in polyatomic resonant ionization spectroscopy and ion-fragment appearance potentials in VUV laser photoionization mass spectrometry. We also plan to extend our work on multiresonant MPI spectroscopic diagnostics for energetic fragments. We are developing new theoretical and experimental methods to study state selected two-photon photofragmentation dynamics. Finally, we are applying laser mass spectrometric techniques to the study of high-temperature unimolecular and bimolecular reactions in energetic systems by means of a pulsed molecular beam pyrolysis source.<sup>33</sup>

## PROGRESS REPORT

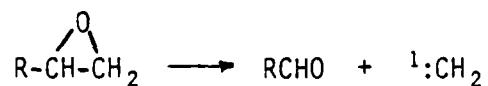
Our program has made substantial progress in its principal area of emphasis -- reaction dynamics of energetic materials. In addition, we have enlarged our scope to address a wider range of problems in molecular spectroscopy and intramolecular dynamics. This latter activity compliments and supports our mainstream effort. It has uncovered sensitive and specific diagnostics for important energetic products, and increased the depth to which we understand the fundamental molecular physics underlying elementary rate processes in energetic systems. In the course of exploring methodologies for generating radical species for diagnostic development, we have also found new methods to apply laser-crossed-molecular-beam techniques to the study of high temperature kinetics in bulk energetic systems. The following sections outline major developments in each of these areas.

## 1. Fragmentation Kinetics and Dynamics of Energetic Reactions

This work applies the technique of infrared multiphoton absorption to excite energetic molecules above thresholds for unimolecular decomposition. The goal is to identify primary fragmentation channels and characterize the kinetics and dynamics of their competition. Our first experiments focussed on the decomposition of nitromethane.<sup>27, 28</sup> Internal state populations and recoil velocities for MPI-detected CH<sub>3</sub> and NO<sub>2</sub> products scattered by laser excited fragmentation from a skimmed pulsed molecular beam led to some preliminary conclusions about exit channel dynamics for this system, but also underlined the need for more sensitive diagnostics. For NO<sub>2</sub> at least this has now been achieved (see below),<sup>21-25</sup> and we are in position for the next generation of experiments on nitroalkanes and nitramines.

At the same time, we have applied existing MPI technologies together with well established techniques in laser induced fluorescence (LIF), to study decomposition systematics and dynamics in another class of compounds, primary alkyl epoxides.<sup>26, 29</sup> These are strained ring heterolytic systems, which are widely used as monomers and have recently been introduced as wide-overhead explosive agents effective in clearing mine fields.

We have established that the principal channel for decomposition of the isolated molecule is methylene elimination:

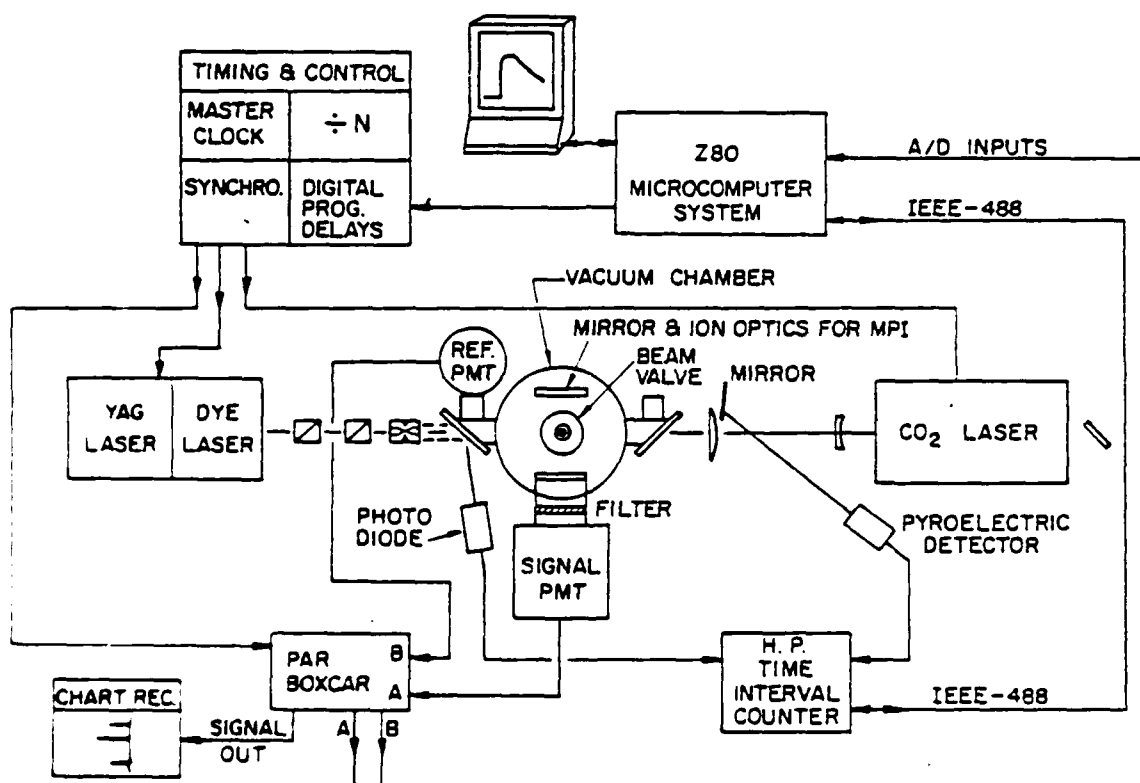


As with our work on nitromethane, we detect products scattered by infrared multiphoton decomposition in a molecular beam by time-, space-, and quantum-state-resolved laser spectroscopy -- multiphoton ionization for the aldehyde and laser induced fluorescence for <sup>1</sup>CH<sub>2</sub>. From the data we obtain information



on dynamics in the form of internal state and recoil velocity distributions, and kinetics in directly measured unimolecular lifetimes.

The set-up of our laser-crossed molecular beam apparatus is diagrammed below



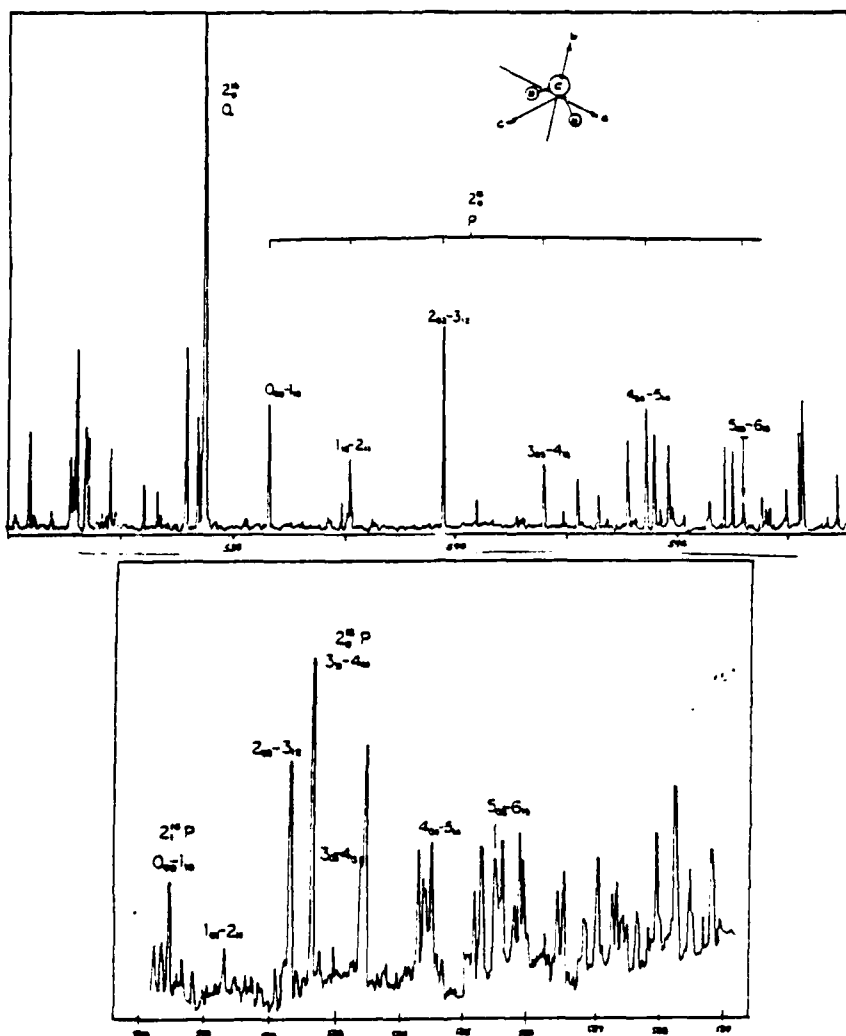
In brief, the experiment uses a pulsed supersonic jet of He, in which is seeded alkyl epoxide ( $R = CH^3$ ,  $C^2H^5$  or  $C^6H^{13}$ ) at a partial density of less

than 0.1 percent. This jet is crossed by the focussed output of a specially designed fast-discharge  $\text{CO}_2$  TEA laser, which produces up to one Joule per shot at 30 Hz with more than 90 percent of the output energy concentrated within a gain-switched pulse of 50 nsec fwhm. A tunable pulsed dye laser probe is aligned to counterpropagate with the IR pump. For LIF, fluorescent emission is collected by an F.1 lens-mirror combination and dispersed by a 0.125 M monochromator for photomultiplier detection. For MPI, the probe laser is focussed. Ions are collected by an electrostatic lens system (which is polished to serve as the LIF-mirror noted above) and detected by a particle multiplier. A laboratory microcomputer acquires the individual signal (LIF or MPI) and measured pump-probe delay for each pair of laser pulses.

In a typical experiment either the delay time is scanned to measure product appearance time or the probe laser wavelength is scanned to take a product spectrum. Product laboratory velocities, from which recoil energy distributions are deduced, are measured by spatially separating pump and probe and monitoring fragment flight times.

That the reaction observed is really  $\text{CH}_2$  elimination from the primary position on the heterocycle is confirmed by isotopic substitution;  $\text{CH}_3\text{CHCD}_2\text{O}$  yields only  $^1\text{CD}_2$ .<sup>26</sup> Isotope specificity, however, fails to answer the question of dynamical pathway. To help decide whether  $^1\text{CH}_2$  elimination is concerted or the sequential product of ring opening followed by C-C (or C-O) scission, we have looked carefully at the spectrum of product states produced by this reaction.

Typical LIF excitation spectra for propylene oxide are shown below.

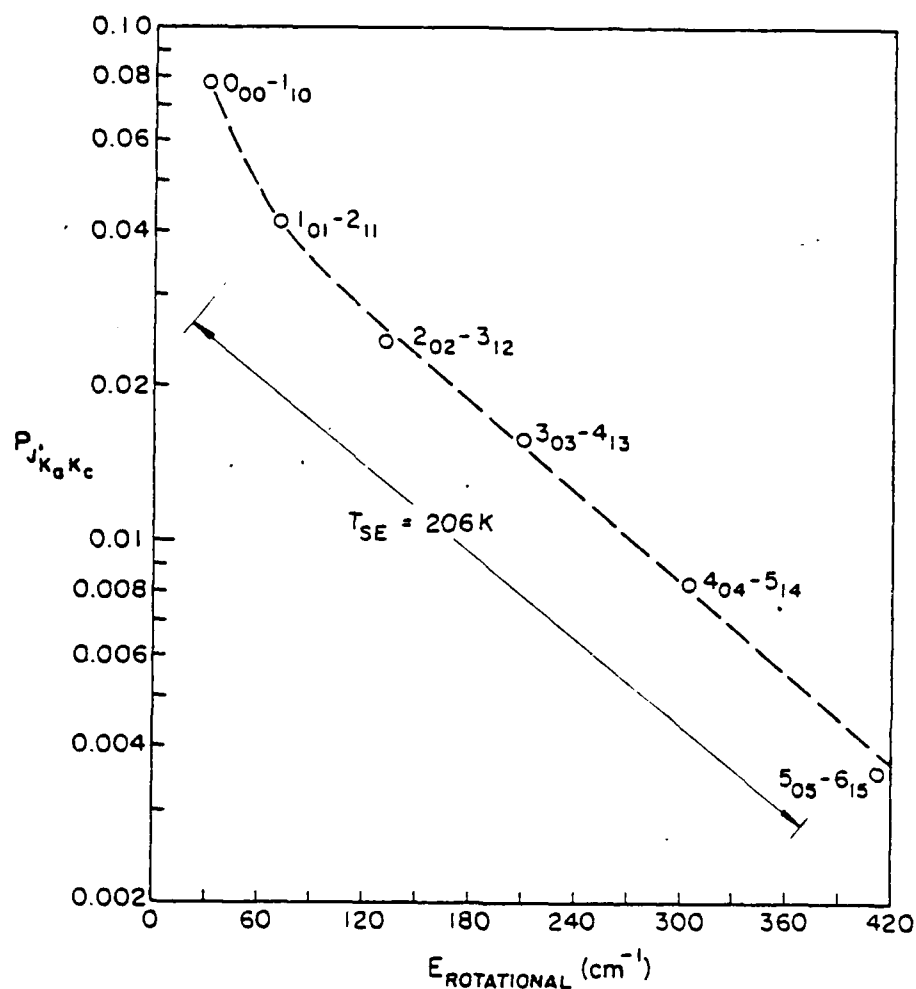


Those found for butyl and octyl epoxide are very similar. Rotational lines in the top frame are labeled with reference to a progression of initial state rotational quantum numbers  $K_a = 0$ ;  $J, K_c = 0, 1, 2, 3, 4, 5$ , where  $J$  refers to total angular momentum and  $K_c$  its projection on the perpendicular axis. These transition intensities thus reflect the population distribution in what might be termed a boomerang mode of rotation.

At lower signal to noise, the bottom frame shows the same rotational sequence for a transition originating from the first excited bending vibration. In both cases spectra are completely unsaturated so that intensities are well related to populations by available Hönl-London factors.

A plot of population per state versus rotational energy for the top

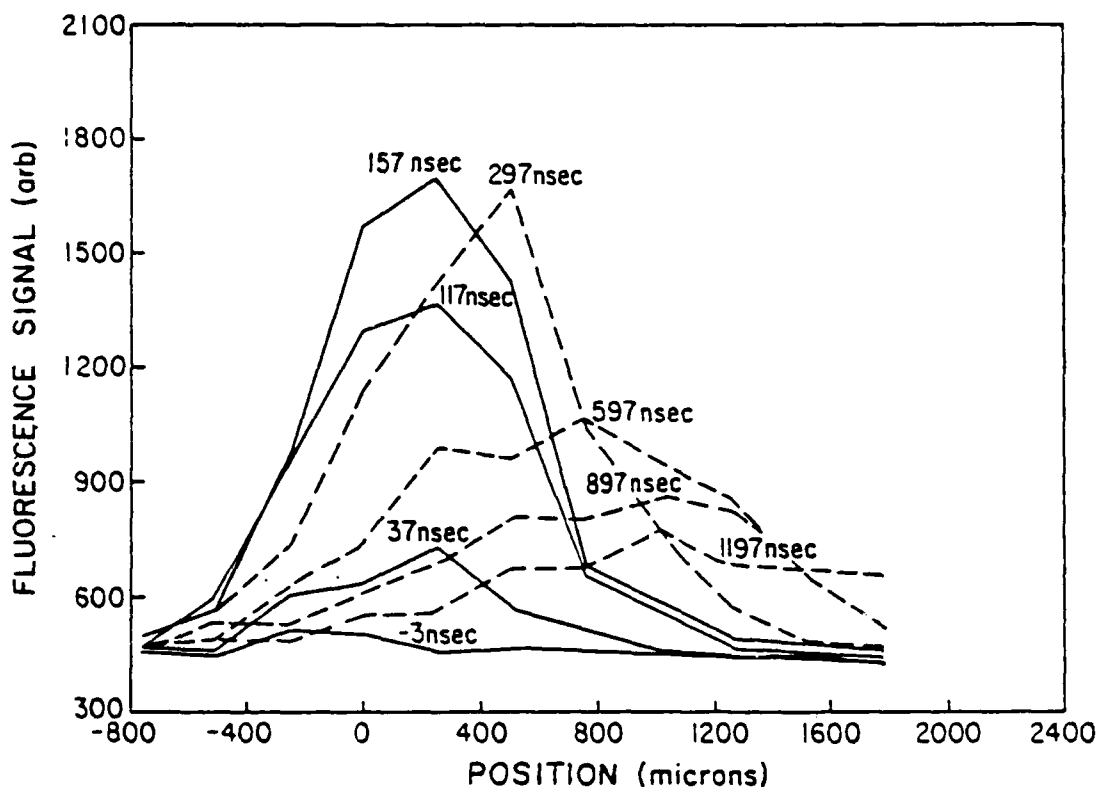
spectrum above is shown below.



As a matter of convenience note that the relative populations are approximately described by a Boltzmann distribution at approximately 200 K. This behavior, including both the approximate temperature and the deviation upward of the rotationless state, is common to all side-chain carbon numbers we have studied and virtually independent of CO<sub>2</sub> laser pulse energy. These results suggest that the decomposition dynamics are a local function of the properties of the heterocycle, and that in the exit channel, these local dynamics favor little CH<sub>2</sub> rotational motion perpendicular to the COC plane. This is most

consistent with concerted molecular elimination.

Data reflecting the time-of-flight distribution of recoiling  $\text{CH}_2$  and  $\text{CH}_3\text{CHO}$  fragments of propylene oxide decomposition are presented below.



These curves show the spatial distribution of  $\text{CH}_2$  along the axis of the beam at various delay times after the  $\text{CO}_2$  laser pulse. The lowest curve, at 37 nsec, was taken while the  $\text{CO}_2$  laser was still on. It gives a snapshot of the spatial distribution of  $\text{CH}_2$  as a convolution of the  $\text{CO}_2$  focal diameter (0.1 mm) and the finite width of the probe (0.5 mm). With increasing time, this instantaneous profile moves downstream with the beam velocity, and

broadens due to the distribution of parent initial velocities combined with the vectorial distribution of recoil velocities. By knowing the initial velocity distribution for our expansion conditions we can estimate the kinetic energy added by fragment recoil.

The same technique is possible for the  $\text{CH}_3\text{CHO}$  fragment using MPI. This provides a confirmation which has even higher resolution because the probe diameter is smaller (focussed to 30  $\mu\text{m}$ ). The laboratory velocities measured for  $\text{CH}_2$  and heavier  $\text{CH}_3\text{CHO}$  are mutually consistent with momentum conservation, yielding a confirmed estimate of the energy deposited in center-of-mass fragment recoil. The results obtained, as summarized below together with numbers characterizing the other sampled dynamical degrees of freedom, show an average recoil energy that is a mild function of IR laser fluence, but small compared with the energy of an IR photon.

TABLE I. Overview of energy disposal dynamics in the infrared laser induced unimolecular decomposition of primary alkyl epoxides

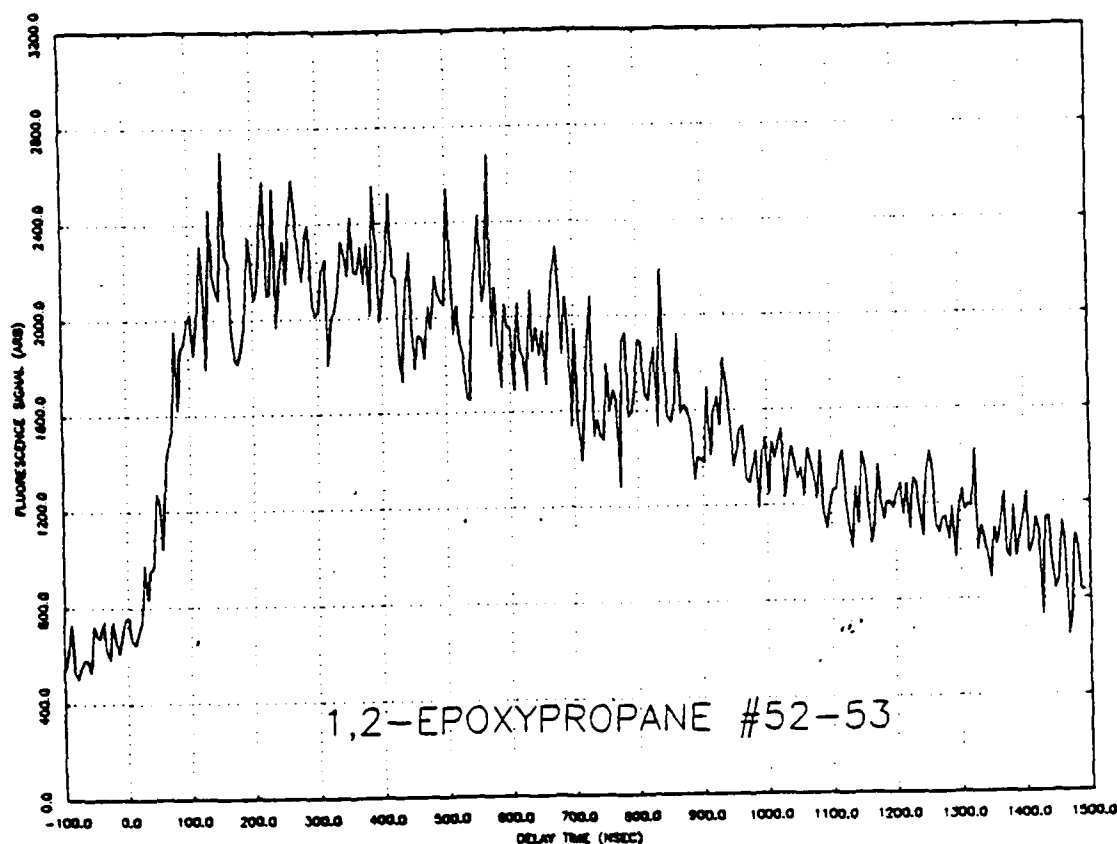
		Fragment [transition]	propyl-	Parent butyl-	octyl-
Rotational dynamics (temp, K)		$\text{CH}_2[2_0^{16}]$	206	209 229	(247)
Vibrational		$\text{CH}_2[\nu_2]$ (1424)		$N_1/N_0 = 0.25$	
Translational velocities (lab, $\text{cm sec}^{-1}$ )					
Fluence	630 mJ	$\text{CH}_2[2_0^{16}]$	$5.9 \times 10^4$	$5.2 \times 10^4$	
	230 mJ	$\text{CH}_2[2_0^{16}]$		$3.2 \times 10^4$	
		$\text{CH}_3\text{CHO}$	$3.4 \times 10^4$		
Recoil Energy (com, $\text{kcal mole}^{-1}$ )			0.8	0.6 0.2	

Taken together these results suggest the picture normally associated with infrared multiphoton dissociation. An ensemble of molecules is excited by sequential photon absorption to levels at some small energy above the lowest dissociation threshold. There decomposition takes place at a rate well determined by RRKM theory. At high pumping intensities the process is characterized by a dynamic competition between dissociation and further up-pumping. Though the point in energy at which these processes become competitive depends on the cross section for photon absorption and molecular complexity (as it effects unimolecular decay rate), the natural assumption seems to have developed that IRMPD is a near-threshold process.

This question of the precise energy distribution of the reacting molecules presents difficulties for the interpretation of IRMPD results for unimolecular kinetics purpose: The confirmation of rate models and even the ordering of thresholds for observed reactions requires some knowledge of the distribution of energy in the field driven ensemble. The fullest understanding of the observed energy disposal dynamics also requires an idea of the average excess energy available in the excited parent. Experiments to date give only indirect information on this distribution. Purely spectroscopic pump-probe investigations measure internal populations in small-molecule fragment degrees of freedom. Molecular beam scattering experiments infer internal energy from recoil velocity distributions.

By both of these conventional measures our alkyl epoxide systems appear to be excited little above the lowest threshold. However, this not-unconventional view of the excitation distribution differs substantially from that provided by another more direct measure of the vibrational energy content of our reacting molecules, the unimolecular decay lifetime. The figure below shows a waveform for  $^1\text{CH}_2$  production from propylene oxide, which is measured

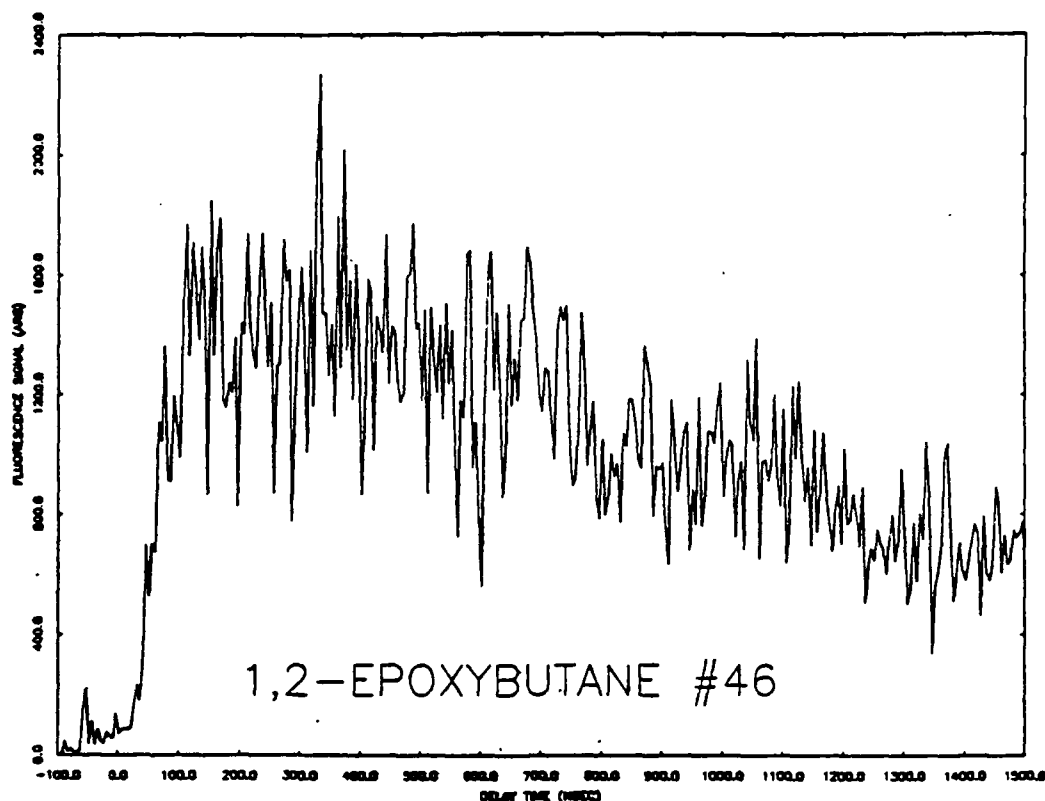
by scanning the delay of the fluorescence probe relative to a  $t=0$  mark furnished by the leading edge of the IR pump pulse.



These measurements are jitter-free; a time interval counter measures the precise delay for every pair of pump/probe pulses. The pump pulsewidth is 50 nsec with a rise time of about 20 nsec. The formation rate of  $\text{CH}_2$  product appears to fall in this same range. Thus, limited by our instrumental resolution, the lifetime of propylene oxide under these conditions is 20 nsec or less. On the basis of RRKM theory, for a molecule of this size to have a lifetime this short requires an excess energy of  $90 \text{ kcal mole}^{-1}$  or 30 IR photons.

A similar risetime is shown below for butyl epoxide.





In this case, by conventional application of statistical rate theory, the rise time observed requires at least  $120 \text{ kcal mole}^{-1}$  above threshold.

These waveforms were recorded under laser power conditions identical to those which produced the spectra and velocity distributions described above. Apparently, either the lifetime of laser prepared alkyl epoxide is anomalously short, or the cold rotational and translational  $\text{CH}_2$  product distributions observed issue from very hot molecules.

The standard theoretical models are not much help in resolving these two possibilities. The fragments are colder than would be expected from phase space theory applied to reactants with the excess energy required by RRKM theory. These are large molecules, however, and such estimates depend precisely on how one counts states. This level of excitation can be made consistent with the usual rate-equations description of the pumping dynamics, but only by invoking a very large IR absorption cross section.

At this point the data appear to support either of two conclusions:

1) Infrared excitation and unimolecular decomposition proceed statistically to produce  $\text{CH}_2$ , on the timescale observed, from a very hot reactant distribution. Dynamical effects in the exit channel contribute, perhaps, to cool the measured rotational and translational product state distributions. Cross sections for infrared absorption by vibrationally excited molecules must be as large as optical cross sections to support this high level of excitation. Or:

2) Infrared cross sections are more normal (like small-signal IR cross sections or smaller), producing a parent excitation distribution more consistent with observed small fragment rotational and translational energies, but parent molecules decompose much faster than statistically predicted. Such a fast decomposition so near the  $\text{CH}_2$  elimination threshold could be facilitated, entirely within the statistical framework of unimolecular rate theory, by an open lower energy fragmentation or isomerization channel that does not yield  $\text{CH}_2$  as a product.

To resolve these possibilities we must know directly the total energy absorbed per molecule. A more complete census of the energy in the products would give us this information. By far the greatest number of unsampled degrees of freedom lie in the aldehyde product. Resonant multiphoton ionization spectra give some information, and work to refine these diagnostics is continuing. In addition, we plan to use appearance frequencies for ion fragments in tunable VUV laser photoionization as a probe of native vibrational energy.

## 2. New Diagnostics for Energetic Fragments

To obtain reliable information on systematics and kinetics in complex energetic systems and to probe scattering dynamics of isolated energetic reactions requires diagnostics that have high sensitivity and high species and quantum state specificity. Work in our laboratory and elsewhere has shown that laser based resonant multiphoton ionization spectroscopies have great potential in this regard,<sup>1-25, 27-31</sup> and we are proceeding with efforts to refine methods based on this approach. In particular, we find the combination of resonant frequency patterns with mass resolution to be a powerful means to confirm fragment identities. Added specificity is gained by newer multicolor-multiresonant methods.<sup>20</sup> Our progress in this area is well illustrated by recent work on two candidate energetic fragments  $\text{NO}_2$  and sym-triazine.

### $\text{NO}_2$ : Non-Franck-Condon Two-Photon Spectroscopy

Two-photon and higher order spectroscopies have long been used to access one-photon forbidden transition systems and, through polarization analysis, provide information key to the assignments of electronic state and vibronic symmetries. Moreover, it has been increasingly recognized that, in two-photon transitions involving real intermediate states, one has an additional dimension that permits the dramatic expansion of Franck-Condon envelopes for molecular electronic transitions. This behavior observed can be traced to state mixing, and is closely connected with ideas of vibrational coupling and IVR (see below).

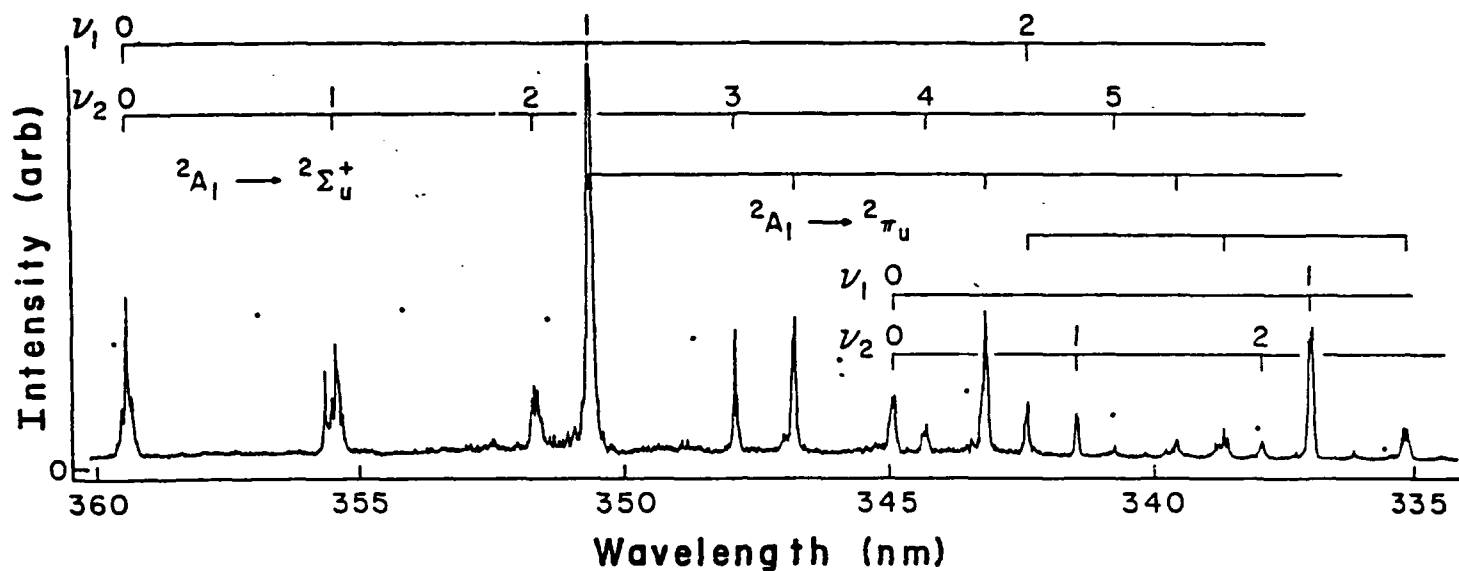
We use perturbations associated with the complex (and dissociative) system of states in the optical spectrum of  $\text{NO}_2$  to facilitate an electronic transi-

tion for which there is a large geometry change. This transition is important to us because the uppermost (Rydberg) state is sharp, simple, readily assignable, and offers clear potential as an important new sensitive and specific diagnostic for this molecule.

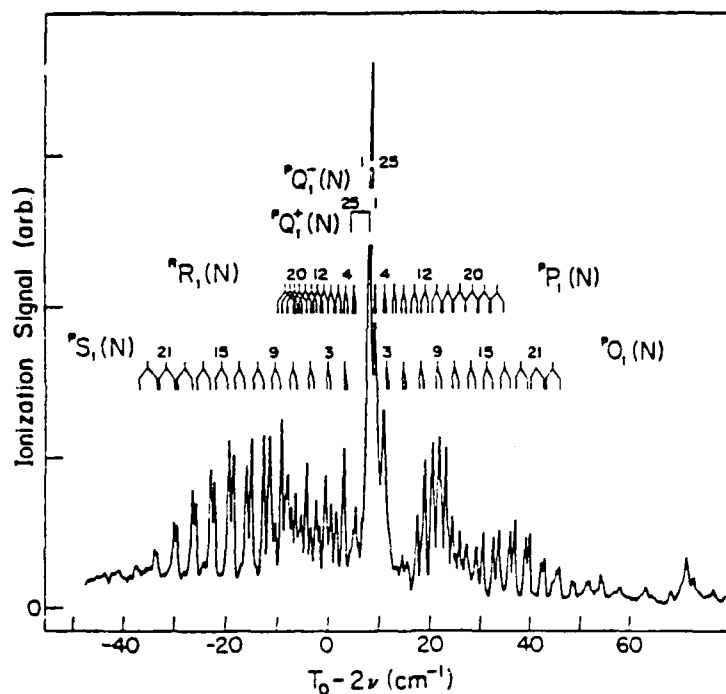
The particular spectroscopic system of interest is that for two-photon transitions from the  $^2A_1$  ground state to Rydberg states lying in the energy region from 55,000 to 65,000  $\text{cm}^{-1}$ . States of  $\text{NO}_2$  in this region have been of experimental and theoretical interest for more than 30 years. Assignment has proven difficult because of the geometry change just mentioned. The 16-electron  $\text{NO}_2^+$  core of the Rydberg states converging to the ground state of the ion is isoelectronic with  $\text{CO}_2$  and thus linear. Transitions from the bent ( $134^\circ$ ) ground state to defining origins either of the Rydberg states or the vibrationless level of the ion are forbidden by vanishingly small Franck-Condon factors.

Our experiments<sup>21,24</sup> reach this electronic band system by two-photon absorption. Resonant at the level of the first photon is a dissociative continuum of states connecting with products  $\text{NO}(^2\Pi)$  and  $\text{O}(^3P)$ . Dissociation competes with two-photon excitation, and in the multiphoton ionization mass spectrum we see both  $\text{NO}_2^+$ , which follows from one-photon ionization of the Rydberg state, and  $\text{NO}^+$ , which comes from three-photon ionization of neutral photoproduct  $\text{NO}$ .

Tuning the mass spectrometer to  $m/e = 46$  we isolate the  $\text{NO}_2^+$ . By then scanning the laser we find the two-photon absorption spectrum of the Rydberg state impressed on the ion signal. This spectrum is shown below.



Here we clearly see vibrationless origin bands and regular progressions in small values of bending and symmetric stretch quantum numbers. The vibrational assignment and symmetry of the upper state is confirmed by analysis of the rotational fine structure. Resolved lines of the origin band are shown below.



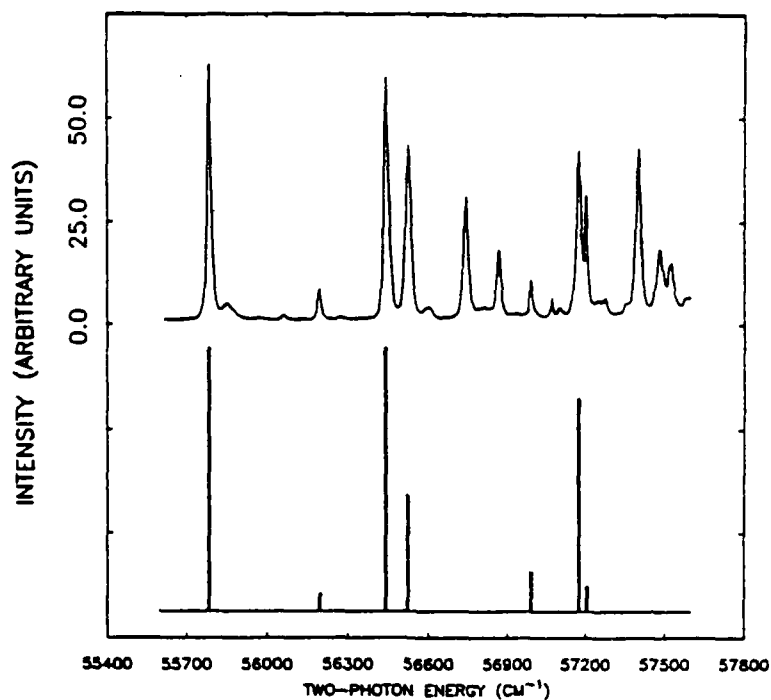
According to this assignment<sup>19</sup> the rotational states of this vibrational level are well described by the linear molecule rotational constant  $B' = 0.419 \text{ cm}^{-1}$ , bending-vibration anharmonicity splitting  $g_{22} = 2.3 \text{ cm}^{-1}$  and spin-rotation coupling parameter,  $\gamma = 0.128 \text{ cm}^{-1}$ .

Origin bands are prominent in this spectrum rather than absent, as would be expected on conventional Franck-Condon grounds, because of the step-wise nature of the two-photon absorption. The two-photon excitation process samples a manifold of dissociative states which are highly mixed with reference to either bent or linear bases. This bridges the Franck-Condon regions for bent and linear states and thus expands the envelope accessible to the electronic transition.

Intermediate dissociation is not a necessary component of this bridging. If we select states in the visible region of the  $\text{NO}_2$  absorption spectrum, we find high transition probability to the Rydberg origins by the absorption of a second, UV photon.<sup>20</sup> Because dissociation is absent, these transitions have much higher ion yield and thus much greater sensitivity. In addition  $\text{NO}_2$  is observed with a simple but very distinctive optical-optical double resonance signature. In either technique, straight two-photon absorption or optical-optical double resonance, we now have powerful laser-spectroscopic means for sensitively and selectively detecting  $\text{NO}_2$ .

#### Dynamical Jahn-Teller Effects in $3s \ ^1E'$ Sym-triazine

The two-photon absorption spectrum of sym- $\text{C}_3\text{N}_3\text{H}_3$  shows a set of sharp vibronic bands associated with a clear origin ( $T_0 = 55,791 \text{ cm}^{-1}$ ;  $55,882 \text{ cm}^{-1}$ ,  $-d_3$ ).<sup>10, 18</sup> These bands, pictured below for triazine- $\text{h}_3$ , are readily assigned to the lowest,  $3s \ ^1E'$ , Rydberg state.



With its totally symmetric Rydberg orbital and degenerate ion core, the limiting separation of cationic and Rydberg electron subsystems<sup>7</sup> predicts this state to be Jahn-Teller active.

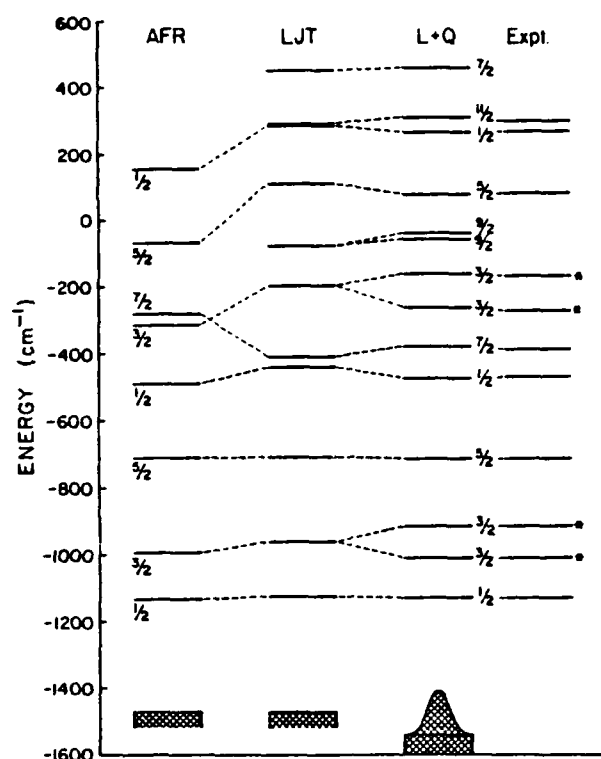
Analysis shows that it is, with coupling dominated by strong activity in a single normal coordinate, the lowest frequency e' mode,  $\nu_6$ , a ring-bending vibration. Comparison of the spectrum above with the appropriate correlation diagram shows that a description in terms of simple linear coupling with  $k \approx 2.2$  (in reduced units of the zeroth-order force constant,  $\lambda$ ) gives a good account of level positions through the conical intersection and above, allowing the confident first-order assignment of all the bands of the spectrum. Linear coupling alone, however, fails to predict the observed intensities (the spectrum shows strong bands which would be forbidden for strictly linear coupling), and certain characteristic splittings. Inclusion of quadratic terms with  $g = 0.046$  and optimization of  $k$  to 2.14 gives quantitative and sensitive agreement with both positions and intensities of all measured bands.

With this coupling strength the zero-point and first few excited levels of the active mode,  $\nu_6$ , lie substantially below the conical intersection. Simple calculation shows that the exact level structure for such conditions is reasonably well described by the eigenvalues of the adiabatic lower-surface Born-Oppenheimer hamiltonian. Motion in these lower states can thus be viewed in very simple terms, as approximately that of a free internal rotor built on a radial harmonic oscillator with a level structure:

$$E(v,j) = \omega(v+1/2) + Aj^2$$

where  $\omega$  is the fundamental frequency and  $A$  is the rotational constant. The latter term is determined by the amplitude of the trough,  $\rho_0 = k/\lambda$ , via  $A = h^2/2m\rho_0^2$ , where for the present case  $\rho_0 = 0.26$  Å and  $A$  is calculated to be  $80 \text{ cm}^{-1}$ . Importantly, it is found that this rotational constant gives a precise account of the deepest few rotor states, so long as the angular momentum quantum number  $j$  is taken to be half-odd integer. This observation constitutes the first direct confirmation of the appropriateness of this form for  $j$ , which can be shown to correspond to a choice of phase in the adiabatic wavefunctions, and as pointed out by Mead, choice of vector potential for the lower surface Born-Oppenheimer or Born-Huang (diagonal) limit as well as for (compensating) off-diagonal terms. It is interesting to note that the energy of the first excited state of this adiabatic-limit pseudorotation is  $160 \text{ cm}^{-1}$ , which corresponds to an extraordinarily low frequency of  $5 \times 10^{12} \text{ sec}^{-1}$  for internal motion in a molecule as rigid as triazine. The level structures predicted by each of the models discussed here are summarized together with experiment below.





This essentially two-parameter fit of the entire spectrum is significant:

1. It offers the most direct and dramatic confirmation yet of the classic theory formulated over twenty-five years ago by Longuet-Higgins and coworkers.
2. It decidedly confirms the strong-coupling (ideal-Rydberg) limit for the interpretation of vibronic structure in molecular Rydberg states; vibration-Rydberg interactions, if present, are beneath the resolution of the correspondence between theory and experiment.

This secure knowledge of the vibronic assignment of sym-triazine provides us with a reliable, vibrationally state-specific diagnostic for this molecule, which has been considered as an intermediate, pyrolytic source of HCN in RDX decomposition.

### 3. Multiresonant Spectroscopy and Intramolecular Dynamics

Questions concerning the nature of vibrational dynamics of highly excited molecules are central to virtually all forms of chemical reactivity, and have been among the foremost subjects of research in the molecular sciences for more than 30 years. Experiments have advanced rapidly in the last decade. Among the most revealing have been studies of laser induced fluorescence in supersonic jets. In such experiments the properties of optically selected vibrational levels of electronically excited states are characterized by means of projection, via emission, to various levels of the electronic ground state. The overall process of optical selection followed by emission can be categorized by the spectrum of the fluorescence. Discrete emission to Franck-Condon active modes of the ground state is termed direct fluorescence. Emission to fundamentals and combinations of inactive modes, which in overall terms can be viewed as a non-Franck-Condon process, is called redistributed or relaxed fluorescence.

This distinction in terms of vibrational states that diagonalize a zeroth-order harmonic hamiltonian, provides a natural basis in which to consider optical transitions. Such transitions select states by their zeroth-order character. An excited level well described by a single harmonic wavefunction will show a vertical emission band, built upon which may be found progressions in successive quantum numbers of totally symmetric modes. A state highly mixed in zeroth-order will show a much more complex spectrum with intensities determined by the amplitudes of the projections of the excited state on each of the zeroth-order (or doorway) states in the basis. Under the proper circumstances such projections can change in time. The evolution of the excited-state wave function from one set of zeroth-order pro-

jections to another defines dynamical intramolecular vibrational energy redistribution (IVR). Thus, in experiment, dispersed (direct or redistributed) fluorescence that evolves in time is evidence for mode to mode IVR.

More fundamentally, excited states can be described in terms of exact molecular eigenstates, states which diagonalize the complete anharmonic hamiltonian. These eigenstates can be expanded in the basis of zeroth-order states. For higher vibrational energies in strongly coupled systems, a large number (say M) of these zeroth-order functions may be required, and thus it can be said that corresponding individual eigenstates are highly mixed. As a consequence, finite projections will exist on many doorway states, and redistributed fluorescence will be in evidence. Taken individually, however, these eigenstates are stationary, and in the absence of expectation or evidence for time evolution, such manifestations of the mixed nature of an excited state must be viewed as a static effect of vibrational (eg. anharmonic, coriolis, nonadiabatic) coupling.

What is actually measured in an experiment, whether static or dynamic IVR, depends on the conditions under which the state is prepared. For example, using an optical pulse of sufficiently narrow bandwidth one can prepare an individual eigenstate. Such a state will show the representative character of its basis modes,

$$|\psi_1\rangle = \alpha|a\rangle + \beta|b\rangle + \dots + \mu|M\rangle,$$

that is direct and, perhaps, redistributed fluorescence but no dynamic IVR. Many experimental examples of this can be found.

By contrast, an excitation pulse  $\phi(t, \omega)$  whose transform bandwidth spans several (say N) molecular eigenstates, will prepare an optically active (doorway) superposition state  $|a\rangle$ :

$$|a\rangle = |\psi(t=0)\rangle,$$

where

$$|\psi(t)\rangle = \gamma(t)|\psi_1\rangle + \delta(t)|\psi_2\rangle + \dots + n(t)|\psi_N\rangle.$$

As this wavepacket evolves it will develop amplitude in projections on doorway states for fluorescence to other modes, and thus show the time dependent emission spectrum characteristic of dynamic IVR. While clear in principle, the direct experimental observation of such real-time evolution has only just been achieved.

Bridging these regimes, it is possible to imagine a process that measures the properties of an isolated (mixed) molecular eigenstate under conditions of narrow coherence bandwidth, transformed to one that, for short times, measures the properties of a zeroth-order mode for excitation with a broad coherence width. The extent of mixing (the size of M) determines the breadth required (size of N) for a pure zeroth-order mode. In the limit of infinite coherence width, the short-time properties measured for the photoprepared state can be expected to match the behavior predicted for an equivalent measurement on the ground state. This is because the vibrational eigenstates of the excited state form a basis in which to expand the ground vibrational state. When this basis is complete, the expansion is exact and we have, by optical projection, an image of the ground state wavefunction in the excited state:

$$|g\rangle = \sum_i |\psi_i\rangle \langle \psi_i | g \rangle$$

The method most often used to prepare such a coherent superposition is to employ a short (psec or sub-psec) laser pulse. However, other means exist to transform broaden an intermediate superposition, which do not depend on the coherence properties of the laser itself. One such alternative approach is to rely on the transition time in a multiphoton excitation, using, in essence, power broadening to introduce a coherence width. This effect has been demonstrated in atoms as manifested by power dependent photoelectron angular dis-

tributions. We have found similar effects of power on relative band intensities in the non-Franck-Condon two-photon absorption spectrum described above. Our experiments probe the character of an optically prepared excited electronic state by second photon absorption. As noted, the second photon absorption spectrum in question shows, by optical projection, that the intermediate state is highly mixed. When we increase the power we change that spectrum. The changes we observe are entirely consistent with the increased coherence width imposed on the pumping process by power broadening. The main significance of these findings is that they illustrate the power of direct optical probing of excited state dynamical processes by state resolved absorption spectroscopy. We plan to extend this work to the application of subpicosecond pulses in time resolved pump-probe Rydberg and photoelectron spectroscopy.

#### 4. Dynamics of State-Selected Two-Photon Photofragmentation

Photoexcitation in the ultraviolet is a well established and widely used technique for promoting molecular fragmentation. For experimental conditions under which nascent product state distributions can be determined free of collisional scrambling, photodissociation techniques can offer substantial insight on the dynamics of primary decomposition processes.

Theory, which ties observed final state distributions with the quantum evolution of a system driven from photoexcitation through dissociation, has made substantial progress in the past few years. It has now become possible to make interesting definite predictions of final state distributions for given initial reactant quantum states for certain simple photodissociation systems. Some of the greatest challenges now remaining are experimental. Theory demands a specified initial state, but it is difficult to select an

individual state from among many when photoexciting to a continuum. The insertion of an intervening step of photoselection overcomes this limitation, and two new two-photon photodissociation techniques have been introduced this year. Both have produced startling new levels of dynamical resolution.

One of these techniques is IR/UV double-resonant photodissociation as developed for  $\text{H}_2\text{O}$  by Andresen and Rothe. The other is optical-optical double resonant two-photon photodissociation developed in our laboratory for  $\text{NO}_2$ .<sup>31, 32</sup> In our work, individual states of  $\text{NO}_2$ 's bound optical absorption system are selected by the absorption of one visible photon. A second photon carries the system above the threshold for  $\text{NO}_2 \longrightarrow \text{NO} + \text{O}(^1\text{D})$ .

The channel to produce excited oxygen is observed to dominate the formation of vibrationally cold  $\text{NO}(X\ ^2\Pi, v=0)$ , which is detected by resonant two-photon ionization. For two-photon photolysis energies within  $100\text{ cm}^{-1}$  of threshold, photodissociation dynamics, manifested in NO rotational and  $\Lambda$ -doublet state distributions, are observed to be a sensitive function of parent intermediate state. NO populations are an oscillatory function of J, with varying patterns of  $\Lambda$ -doublet preference that change with selected  $\text{NO}_2$  intermediate state.

Work described above on the optical-optical double resonance spectroscopy of  $\text{NO}_2$  Rydberg states offers a means of assigning intermediate features of interest in these photodissociation experiments. In particular, from OODR rotational fine structure we should be able to clearly define intermediate angular momentum. We expect that such information coupled with new theoretical models for photodissociation, which explicitly include electronic degrees of freedom, can be expected to help unravel the complicated and interesting patterns of energy disposal obtained in these and similar experiments, as well as improve understanding of the visible spectrum of  $\text{NO}_2$ .

5. Thermal Unimolecular Kinetics by Pulsed Molecular Beam Pyrolysis

Laser induced fluorescence and ionization spectroscopies coupled with free jet expansions can yield detailed structural information on atomic and molecular free radicals, which is important for both fundamental and diagnostic purpose. Such methods generate radicals in a nozzle and entrained them in a supersonic expansion of inert gas. This effectively isolates reactive species from chemical decay, while cooling internal degrees of freedom to near absolute zero, greatly simplifying spectra.

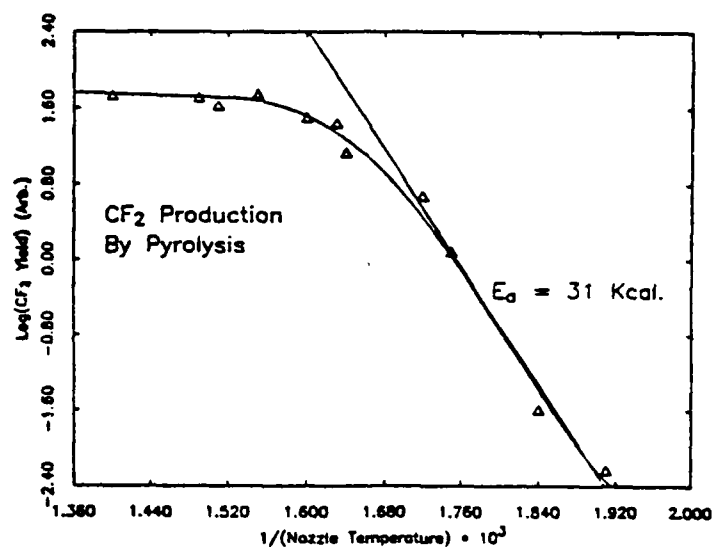
We have worked to develop new methods for the jet-production of radical species of interest for energetic materials. A component of this work has investigated thermal pyrolysis of suitable precursors in the throat of a pulsed jet as a means of producing beams of selected atomic and molecular radicals. The success of this method holds additional promise as an interesting new means for studying the kinetics fast primary and secondary reactions in high temperature thermal pyrolytic systems.

Preliminary kinetics studies demonstrating feasibility have been conducted for a wide range of systems. By the method of jet-pyrolysis, we have succeeded in generating a number of interesting atomic and molecular radical species. In addition, we have established that this technique offers promise as well for the study of the fast kinetics of high temperature reactions in energetic systems.

Thus far we have explored the feasibility of pulsed pyrolysis as a means of studying primary thermal unimolecular kinetics for a range of compounds including alkyl nitrites, halocarbons, and organometallics. Researchers at Exxon Corporate Research Laboratories have extended our techniques to study the pyrolysis of hydrocarbons.

In all applications, decomposition of the parent molecule occurs as the reactant mixture passes through a heated nozzle on its way from a pulsed molecular beam valve into a high-vacuum chamber. Products are detected by laser induced fluorescence or multiphoton ionization.

Typical data are illustrated below for  $\text{CF}_2$  produced in the pulsed thermal decomposition of hexafluoropropene oxide.<sup>33</sup>



Yield as a function of nozzle temperature at first follows an Arrhenius dependence returning an activation energy very close to that measured by conventional thermal decomposition experiments. At very high temperature the yield of  $\text{CF}_2$  appears to saturate. From the known thermal Arrhenius parameters for this reaction, we calculate the rate at this break-over to equal the average residence time of the gas in the nozzle (as determined by the pulse-shape of the beam). This suggests that the  $\text{CF}_2$  yield ceases to increase because all the parent has decomposed. Comparison of the absolute  $\text{CF}_2$  density, as measured by saturated fluorescence, with the known amount of hexa-



fluoropropene oxide initially present in the pulse, confirms this.

As outlined below, we have plans to modify this technique to improve kinetic resolution. We will lengthen the time the gas pulse is at high temperature while shortening the voiding time of the reservoir, by increasing the hot nozzle diameter and fitting it with a fast shutter.

In addition to studies of primary thermal kinetics, we expect this technique will find utility in laser-probed secondary reaction kinetics involving mixtures of energetic reactants and additives.

## REFERENCES

1. R. J. S. Morrison and E. R. Grant, J. Chem. Phys. 77, 5994 (1982).
2. B. H. Rockney, G. E. Hall and E. R. Grant, J. Chem. Phys. 78, 7124 (1983).
3. R. L. Whetten, K. J. Fu and E. R. Grant, J. Chem. Phys. 79, 4899 (1983).
4. R. L. Whetten, K. J. Fu and E. R. Grant, J. Chem. Phys. 79, 2626 (1983).
5. R. L. Whetten, K. J. Fu and E. R. Grant, J. Phys. Chem. 87, 1484 (1983).
6. R. L. Whetten and E. R. Grant, J. Chem. Phys. 80, 1711 (1984).
7. R. L. Whetten and E. R. Grant, J. Chem. Phys. 80, 5999 (1984).
8. R. L. Whetten, C. E. Otis, K. J. Fu, and E. R. Grant, Proc. Intl. Conf. on Radiationless Transitions, Newport Beach, CA, January 1984.
9. R. L. Whetten, G. S. Ezra, and E. R. Grant, Proc. Intl. Conf. on Radiationless Transitions, Newport Beach, CA, January, 1984.
10. R. L. Whetten and E. R. Grant, J. Chem. Phys. 81, 691 (1984).
11. S. G. Grubb, R. L. Whetten, A. C. Albrecht, E. R. Grant, Chem. Phys. Lett. 108, 420 (1984).
12. R. L. Whetten, K. J. Fu and E. R. Grant, Chem. Phys. 90, 155 (1984).
13. R. L. Whetten, S. Grubb, C. E. Otis, A. C. Albrecht and E. R. Grant, J. Chem. Phys. 82, 1115 (1985).
14. S. G. Grubb, C. E. Otis, R. L. Whetten, E. R. Grant and A. C. Albrecht, J. Chem. Phys. 82, 1135 (1985).
15. R. L. Whetten, G. S. Ezra and E. R. Grant, Ann. Rev. Phys. Chem. 36, 277 (1985).
16. J. W. Zwanziger, R. L. Whetten, G. S. Ezra and E. R. Grant, Chem. Phys. Lett. 120, 106 (1985).
17. R. L. Whetten and E. R. Grant, J. Chem. Phys. 84, 654 (1986).

18. R. L. Whetten, K. S. Haber and E. R. Grant, J. Chem. Phys. 84, 1270 (1986).
19. M. B. Knickelbein, K. S. Haber, L. Bigio and E. R. Grant, Chem. Phys. Lett., submitted.
20. L. Bigio and E. R. Grant, to be published.
21. R. S. Tapper, R. L. Whetten and E. R. Grant, J. Phys. Chem. 88, 1273 (1984).
22. L. Bigio, R. L. Whetten, R. S. Tapper, and E. R. Grant, Proc. Intl. Conf. on Radiationless Transitions, Newport Beach, CA, January, 1984.
23. L. Bigio and E. R. Grant, Israel J. Chem. 24, 251 (1984).
24. L. Bigio and E. R. Grant, J. Chem. Phys. 83, 5361 (1985).
25. L. Bigio, G. S. Ezra and E. R. Grant, J. Chem. Phys. 83, 5369 (1985).
26. J.-S. J. Chou, T. E. Adams and E. R. Grant, J. Chem. Phys. 77, 1886 (1982).
27. B. H. Rockney and E. R. Grant, J. Chem. Phys. 77, 4257 (1982).
28. B. H. Rockney and E. R. Grant, J. Chem. Phys. 79, 708 (1983).
29. T. E. Adams, M. B. Knickelbein, D. A. Webb and E. R. Grant, Proc. NATO Advanced Study Institute on Fast Processes in Energetic Systems, Iraklion, Crete, August, 1985.
30. R. S. Tapper, L. Bigio, and E. R. Grant, J. Phys. Chem. 88, 1271 (1984).
31. L. Bigio and E. R. Grant, J. Phys. Chem. 89, 5855 (1985).
32. L. Bigio and E. R. Grant, Proc. Intl. Laser Science Conf., Dallas, Texas, November, 1985.
33. M. B. Knickelbein, D. A. Webb and E. R. Grant, Materials Research Society Proceedings, "Synthesis and Etching Electronic Materials", T.P.H. Chang, Ed. (North-Holland, New York, 1985), p. 23.

**PARTICIPATING SCIENTIFIC PERSONNEL**

Past Personnel with Degrees Conferred

Robert L. Whetten (NSF Fellow)	Ph.D., 1984
Dr. Fu Ke-Jian	(Visiting Scientist)
Rochelle Tapper	B.S., 1983

Present Personnel

Laurence Bigio  
Douglas Webb  
Kenneth S. Haber

END

DTIC

7-86